Computer Science Department Technical Report
University of California
Los Angeles, CA 90024-1596

QUANTITATIVE MODEL OF THE VERTEBRATE CONE RECEPTIVE FIELD

J. Skrzypek
G. Wu

October 1992
CSD-920048

1 Introduction

The idea that the retinal output contains second order, spatial difference of the input such as Laplacian of intensity was first introduced by Mach in 1868. Kuffler (1953) extended this hypothesis by finding cat ganglion cells that encode spatial difference of intensities through antagonistically organized, concentric receptive fields. Ratliff (1965) related Mach's spatial derivative with the retinal mechanism of lateral inhibition. At the same time Rodieck and Stone (1965) reported that cat ganglion cells with the antagonistic, center-surround receptive fields (RF) can be modelled as a difference of two concentric Gaussian sensitivity profiles; difference of Gaussians - DoG. Marr and Hildreth (1980) were first to propose Laplacian of a Gaussian (LoG) as a generic analytical model for isotropic RF. They argued that Gaussian is useful in reducing noise and the Laplacian can accurately localize intensity discontinuities; LoG filter, can be modelled by a DoG operator when the diameter of center Gaussian is approximately one third of the *surround* Gaussian.

In the past twenty years, the concentric organization of RF's into antagonistic zones was reported in bipolar cells (Werblin & Dowling, 1969), in horizontal cells (HC's) (Skrzypek, 1984; Skrzypek & Werblin, 1983) and in cones (Baylor, Fuortes, & O'Bryan, 1971; Skrzypek & Werblin, 1983; Skrzypek, 1990b). It is now well established that antagonism begins with cones (Skrzypek & Werblin, 1983; Baylor et al., 1971; Burkhardt, 1977) but the quantitative comparison of DoG or LoG formalism with actual physiological data has never been performed. We report here such comparisons using intracellular data from the cone and HC's in the eyecup preparation of the Tiger salamander retina. The data from physiological experiments is used to build a simulation of the outer plexiform layer (OPL) of retina that

is equivalent to 128 by 128 array of cones.

Several new findings emerged requiring modification to DoG model of receptive field as applied to retinal cones. The results suggest a more accurate approximation of the cone RF as compared to DoG is the difference between central Gaussian (G_c) and the sum of *displaced surround Gaussians* (G_s). The G_c represents the RF of a cone and it reflects the coupling between neighboring receptors. The G_s represent combined RF's of HC's within immediate vicinity of a cone; the sensitivity profile of G_s resembles an annulus, the complete center-surround assembly resembles the Difference-of-offset-Gaussians (DooG) model(Young, 1987) with some modifications. Our model predicts that feedback from HC to a cone that is concentric with HC's perikaryon is very weak. The feedback is an integration of synaptic inputs from the HC's dendritic fields (DF's) that are displaced laterally with respect to the cone.

2 Materials and Methods

Preparation and the general experimental procedure were described previously in detail (Skrzypek, 1984; Skrzypek & Werblin, 1983). Briefly, all experiments were performed using eyecup preparation from the Tiger salamander. Intracellular recordings were made with single or double barrel micropipettes filled with 4M potassium acetate. For staining experiments, one of the two barrels was filled with 3% solution of Lucifer Yellow dissolved in 1M LiCl. Cones were identified on the basis of physiological criteria (Werblin & Dowling, 1969; Kaneko, 1970; Lasansky, 1981) and later confirmed by staining with Lucifer yellow (Stewart, 1978). Light stimuli were generated by specially constructed double-beam photostimulator

which could deliver concentric, circular and annular stimuli of white or monochromatic light. The flux density of the unattenuated light on the retina was about 15 mW/cm^2.

Several criteria were used to distinguish cones from other cells in the OPL. First of all, the depth of recording in the retina (Kaneko, 1970) at which the cone was penetrated was correlated with histological evidence, as corresponding to the layer of cone inner segments. It also appears that at this depth, the only other cell bodies belong to rods (Lasansky, 1978). After recording from a cone, further advancement of electrode sometimes resulted in penetration of a rod. On the other hand, after recording from bipolar cell, further advancement of electrode always produced penetration of a horizontal cell followed by rods or at times cones. This sequence of penetrations concomitant with characteristic light responses was a very useful heuristic in differentiating cones from bipolars. One exception are cone pedicles, which could be penetrated and mistaken for bipolar cells, especially, if other impalements were to follow. Hence, it is important to emphasize that no single test alone could be used to differentiate cones from bipolar cells and only a sequence of tests followed by staining could give reasonable indication of the penetrated cell type. The identification of single cones was also based on spectral response curves. For the red cones, the only ones considered in this study, their peak in wavelength spectrum, fit well with absorption spectrum for red pigment (Attwell, Werblin, & Wilson, 1982). The spectrum response curve for HC or bipolar cells were often flat or even peaked in the short wavelengths (Skrzypek, 1990b; Skrzypek & Werblin, 1983; Skrzypek, 1984). Cones as compared to horizontal cells or bipolars, had smallest diameter for RF center < 0.075 mm (Marshall & Werblin, 1978). The average for bipolars was about 0.15 mm and the smallest horizontal cells were found to be about 0.3 mm. Under dark adapted conditions cones were also distinguished by the fastest time from dark

the peak of the light response (50 ms) as compared with bipolars (100 ms) or horizontal cells (>150 ms). One additional criterion was that the I-R curves for cones usually span 3 - 4 log units (LU) of intensity between 5% and 95% of the saturating membrane potential value. On the other hand the I-R curves in bipolars were found to span on the average 1 LU (1.3 LU in mudpuppy (Werblin, 1978)). These values represent averages derived from all intracellular recordings in 37 cones, 84 bipolar cells, more than 1000 horizontal cells, and more than 100 rods.

In some experiments the attempt was made to stain the physiologically identified cones and other cells with Lucipher yellow. A good staining was considered when the response of a cone did not deteriorate by more than 20%. Often, the center-surround antagonism would disappear or decrease significantly so that we could not complete the measurements of dynamic changes in I-R curves, but we could still record an unchanged center response. In most of these cases we attempted to fill the cone with the stain. The stained cells were viewed immediately after injections, under epifluorescent microscope, without going through conventional procedures of fixating and embedding tissue (Skrzypek, 1984). While the stained HC and bipolar cells always showed extensive arborization of dendritic processes, protruding from the soma, this was not the case for cones which appeared as symmetrical spheres. In all 37 cones were identified by a combination of these criteria and partial results were obtained in most cases, including 19 attempts at staining. In six of these cells the experiments were completed but only in three of the six the staining was also successful. Out of 117 attempts to stain HC's, 31 resembled axon terminals without clear perikaryon and were associated with very large RF's. The remaining 86 had classical appearance of the cell body with numerous fine dendrites and often stained in clusters of between two and six.

Many of these HC's had their RF centers between 0.3 mm and 1 mm and could be made to display center-surround antagonism.

3 Results

3.1 Center-Surround Antagonism in Cones

Although the organization of the cone RF into antagonistic zones of center and surround has been firmly established in lower vertebrates (Baylor et al., 1971; Skrzypek & Werblin, 1983, 1978; Werblin, 1978; Lasansky, 1981) an explicit model of this organization is still lacking. Fig. 1 shows series of light responses recorded intracellularly from the red cone. White spot of light (0.15 mm at -3 LU) evoked, near saturating, peak hyperpolarization of about 20 mV measured from the resting membrane potential in the dark of V_m = - 40 mV; there is little change during the plateau portion of the response. However, the response waveform changed drastically when the diameter of the stimulus was increased to 1 mm. Although the peak response and the onset time-course remained unchanged, the plateau portion of the response showed 30% depolarization from -61 mV to -54 mv as compared to peak response. The time course of this depolarization was much slower than the onset of the hyperpolarizing response, culminating with a clear transient undershoot when the stimulus was turned off. This slow onset of depolarization reflects integrated delay caused by peripheral signal traveling from increasingly eccentric areas of the retina. This result agrees well with similar observation in turtle and fish retinae and it demonstrates that in the intact retina the waveform of the cone light response can be represented as a function of the stimulus diameter; illumination of peripheral area of RF antagonizes the effect of the stimulus in the center of RF.

[Insert Fig. 1 About Here]

Fig. 2 shows the cone light response plotted as a function of the stimulus diameter. The peak V_m of the response (crosses) increased to a maximum value at the spot diameter of about 0.1 mm. However, during the plateau, measured one second after the peak response, the V_m (filled squares) decreased drastically from 9 mV at 0.1 mm down to 3 mV at 2 mm, the maximum diameter stimulus covering the whole eyecup preparation.

[Insert Fig. 2 About Here]

The plot of the peak response can be fitted by integrating a Gaussian curve $G_c = A_c \exp^{-(\frac{r}{r_c})^2}$, where r_c (0.05 mm) is the radius of the cone RF center, r is the distance from the long axis of the cone and the A_c is the gain coefficient for the center of RF, assumed to be one. The result in Fig. 2 argues against modelling cone RF as a Laplacian of a Gaussian (LoG) function. Laplacian of central G_c with 0.1 mm diameter predicts that the strength of antagonistic surround will diminish to zero at approximately 0.15 mm from the center of RF (Fig. 3 and Fig. 4). The data in Fig. 2 shows strong antagonism even when the radius equals 1 mm. In addition LoG function specifies the amplitude of the center to be fixed at exactly twice the amplitude of the antagonistic surround (Fig. 3) which can not be fitted against the plateau curve in Fig. 2. This suggests that cone RF is not balanced between its center and surround zones and consequently can not and does not behave as a zero crossing detector.

A better model is the traditional DoG function (Rodieck, 1965). The balance between G_c and G_s is described by the filled circles curve (Fig. 2) that can be fitted by $DoG = G_c - G_s = A_c \exp^{-(\frac{r}{r_c})^2} - A_s \exp^{-(\frac{r}{r_c})^2}$ where $r_c = 0.025$ mm, $r_s = 0.5$ mm, $A_c = 1$ and $A_s = 0.037$. This

analytical model gives only approximate fit because it shows that at radius value of 50 μm, cone membrane potential (V_m) for both peak and plateau should be approximately equal. However, data in Fig. 2 shows that even at 0.1 mm of the stimulus diameter, the feedback is strong enough to decrease the plateau response to about 70% of the peak response. A fraction of this decrease could be due to light adaptation process that is not being captured in the analytical model. But in general, the decrease indicates unbalanced center and surround contributions.

[Insert Fig. 3 About Here]

[Insert Fig. 4 About Here]

The DoG model (Fig. 3 and Fig. 4), assumes that the G_s is spatially continuous and concentric with G_c of cones and that it can extend from 0.3 mm to 2 mm (Skrzypek & Werblin, 1983; Skrzypek, 1984); spatial continuity of G_s results from electrical coupling between HC's(Skrzypek & Werblin, 1983). This assumption can not be easily reconciled with the observation that HC's display center surround antagonism (Skrzypek & Werblin, 1983; Skrzypek & Werblin, 1978).

3.2 Center-Surround Antagonism in Horizontal Cells

Fig. 5 shows a series of intracellular recordings from the *narrow field* HC in response to center spot of light (0.5 mm) and the concentric annular illumination (ID = 1 mm and OD = 2 mm). The peak response of this HC reaches maximum at stimulus diameter of about 0.6 mm, the extent of the RF center (Fig. 6). The intensity of the annulus was fixed at -3.2 LU and when presented alone it caused the small (5 mV) hyperpolarizing response, probably

because of light scatter from the annulus to the center. Apparently the amount of scatter is sufficient only to excite rods input to the HC; at the stimulus offset, the V_m of this HC returns slowly to the dark resting potential (-31 mV) with a time course characteristic for rods. In the presence of center spot of light with increasing intensity, the hyperpolarizing *surround* response reverses in polarity and becomes depolarizing at center spot intensity of -4.5 LU. Here, the overall time course of the center response still retains the slow recovery to dark V_m level suggesting predominance of rod input (Marshal & Werblin 1978). Further increase of the center intensity, up to -3.5 LU, depresses the depolarizing surround response to zero, concomitant with a change in the time course of the center - light elicited response at the offset, indicating cone input. The depolarizing surround response can be restored to the previous level by increasing center spot intensity up to 2.5 LU. But further increases eliminate the surround response again.

[Insert Fig. 5 About Here]

The changes in center-surround antagonism with increasing center intensity have been observed in many *narrow field* HC's(Skrzypek, 1979). They seem to be related to rod-cone differences in synaptic transmission to HC and will be addressed elsewhere (Skrzypek, in prep.). The final decrease in the mechanism of surround depolarization at center intensities of -2 LU (Fig. 5) was suggested to result from decreasing feedback conductance associated with the reversal potential of -65 mV; the closer the center elicited hyperpolarization brings the cone's V_m to -65 mV the smaller the effect of any changes in feedback conductance on membrane potential(Skrzypek & Werblin, 1983; Skrzypek, 1990b).

The results in Fig. 5 suggest that antagonistic effect of surround measured previously in cones can be also seen in some HC's. This has been previously explained as a natural consequence of HC being postsynaptic to cones and reflecting their activities(Skrzypek & Werblin, 1983). The antagonism observed in HC can be seen at different levels of stimulus intensity without any effect on the size of RF center. Fig. 5 shows plots of the HC responses as a function of the stimulus diameter at different intensity of the spot. The resting potential of this cell in the dark was -25 mV. The size of RF center is defined here as a diameter at which the plateau response reaches maximum hyperpolarization; this corresponds to the first knee on all curves with open symbols, which is about 0.5 mm. The strength of the center-surround antagonism, seen in the individual HC's (Fig. 6) does not seem to be affected greatly by the intensity of the stimulus, when measured as a function of increasing spot diameter.

[Insert Fig. 6 About Here]

The results in Fig. 5 and Fig. 6 argue against a simple DoG function as a model for the cone RF. DoG requires that the response measured from the HC in the center of RF be maximally hyperpolarizing which is inconsistent with the observation that HC's display depolarizing surround responses to annular illumination. These results suggest that HC's do not feedback strongly to cones concentric with the center of their dendritic fields.

4 Simulation

4.1 Center-Surround Antagonism in Cones is Best Approximated by the m-DooG Model

To explain the changes in cone response versus stimulus size, we first considered the several classical RF models, including Difference-of-Gaussians (DoG)(Rodieck, 1965), Laplacian-of-Gaussian (LoG)(Marr & Hildreth, 1980), Gabor(Daugman, 1980), Difference-of-Exponentials (DoE), and Difference-of-Offset-Gaussians (DooG)(Young, 1985). The DoE model is qualitatively undistinguished from the DoG model based on their Fourier transforms and the Gabor model is clearly inappropriate due to the multiple sidelobes in its sensitivity profile that are not consistent with available data. Thus, we examine only DoG, DooG, and LoG in detail.

After simulation studies of the three models (LoG, DoG, and DooG), we found that a modified form of the the DooG RF model accounts best for both physiological and anatomical data. The classical RF models implicitly assume that functions based on difference of Gaussians capture all salient RF properties. While the central portion of the cone RF, mediated by electrical coupling among neighboring cones, are often satisfactorily modelled using a Gaussian, the surround portion of the cone RF, mediated by HC dendritic field (DF) and electrical coupling among neighboring HC's, does not seem to be adequately characterized by a simple Gaussian(Wässle & Boycott, 1991).

What synaptic arrangement would allow the same HC to receive inputs from cones and also to feedback to some of them without balancing out the feedforward and feedback effects?

Such a scheme is possible if we imagine that the strength of feedback to cones within the HC's DF is minimal at the HC's perikaryon and increases with eccentricity from the center of DF. In the rhesus monkey retina(Kolb, 1974; Wässle & Boycott, 1991) some peripheral HC's that make up to 50 contacts with 10 to 12 cones show no contact with pedicles concentric with HC soma. Where HC contacts were observed, less than 10% (5 out of 50) of all contacts with one cone pedicle belonged to a HC whose perikaryon is concentric with a given cone. This suggest that most of the contacts must come from HC's whose cell bodies are laterally displaced with respect to the cone. Conversely, it suggests that only 10% of the total feedback signal strength to a cone pedicle comes from the HC whose soma is concentric with the pedicle. In other words, the sensitivity profile of the feedback signal appears to resemble an inverted-Gaussian or a bimodal distribution (e.g. the sum of 2 Gaussians that are laterally displaced with respect to the central cone). It would also seems that HC's are not the only retinal cells to have this RF characteristic but also the cholinergic amacrine cells(Wässle & Boycott, 1991).

[Insert Fig. 7 About Here]

Fig. 7 schematically outlines the decomposition of the examined RF models into Gaussian and inverted-Gaussian bases. The functional connectivity diagram of the OPL is shown on the left. Three types of shaded arrows illustrate different synaptic pathways that underly various components of receptive fields in cones and horizontal cells. The Gaussian sensitivity profile of the cone RF center and surround components modeled by the DoG function is shown in Fig. 7.A. Here both Gaussians are simply convolved using a kernel indicated by the black rectangle; black corresponds to filled arrows indicating feedback pathway. The

rectangle represents the uniform spatial distribution of feedback from HC to cones.

The sensitivity profile of the DooG model (Young, 1987) for the second order Gaussian derivative consists of an excitatory central Gaussian basis and two laterally displaced inhibitory Gaussian bases. All Gaussian bases have the same space constant and the overall center-surround contribution is balanced (Fig. 7.B). This standard model has several limitations and must be modified to explain our data (hence, modified DooG). First of all, the contribution of the inhibitory offset Gaussians in the standard DooG RF model is uniform everywhere with the exception of the "*hole*" at the center (Fig. 7.B). Second of all, the center-surround contribution is balanced, and finally, all Gaussian bases have the same space constant. To overcome these limitations we model the surround contribution as a weighted sum of offset Gaussians as shown in Fig. 7.C. Here the feedback results from convolving cone and HC's signal using kernel (black) that resembles an inverted-Gaussian.

We will first describe our computational model; the analytical foundation is presented in Appendix A. The simulation results for the four RF models (DoG, LoG, DooG, and m-DooG) are discussed in detail in subsequent section.

4.2 Computational Model of the OPL

Analytical model of the spatial antagonism in cone RF mediated by HC's is based on established experimental evidence and is formalized in Appendix A. However, the analytical model does not allow easy correspondence between behavior and the underlying biological substrates that it represents. Thus, the primary goals of the OPL computational model are (1) to capture the salient features of desired RF models based on existing analytical foundation and known anatomy and physiology and (2) provide an efficient and testable model

that is not bogged down by unnecessary details. As such, a single general model architecture based on the analytical foundation is used with minor changes for the various RF models examined.

The computational model structure (Fig. 8) consists of two layers representing cone pedicles and the type I (narrow field) HC soma. The HC axon terminal (AT) is not included in our model; type I HC AT appears to contact only rods in the primate retina(Wässle, Boycott, & Röhrenbeck, 1989). Also, it is unlikely that any signal interaction exists between the soma and AT because the length and diameter are incompatible with passive electrotonic signal conduction(Gallego, 1983). In our model, each pedicle makes electrical contacts with immediate neighboring pedicles and is driven without any attenuation by the cone outer segment. Most of the negative feedback comes from surrounding HC's. It is implicitly assumed that the cone outer segment compresses the scene illuminance via a logarithmic transform. This assumption is reasonable since light adaptation effects are insignificant in the illuminance range used in the simulations. HC's receive only excitatory inputs from the cone pedicles and are coupled electrically to neighboring HC's. Both pedicle and HC models incorporate *leaks* associated with energy loss in the system, reflecting dynamics of the membrane time constant. The normalized Gaussian and inverted-Gaussian bases of varying spatial extent are used to form all RF's.

[Insert Fig. 8 About Here]

Qualitatively, the negative feedback connections from neighboring HC to a cone serve to remove *locally* redundant components in the respective cone output while preserving signal integrity. The functional view of the model is shown in Fig. 8 and its formalism is shown in

equations 1 through 4.

$$
\begin{aligned}
O_c(t+1) &= ORF(ICF(G_{l\rightarrow c1}, G_{l\rightarrow c2}, S_{l\rightarrow c}) + ICF(G_{c\leftrightarrow c1}, G_{c\leftrightarrow c2}, S_{c\leftrightarrow c}) - \\
&\quad ICF(G_{hc\rightarrow c1}, G_{hc\rightarrow c2}, S_{hc\rightarrow c}) - L_c O_c(t) - K_c) \qquad (1)\\
O_{hc}(t+1) &= ORF(ICF(G_{c\rightarrow hc1}, G_{c\rightarrow hc2}, S_{c\rightarrow hc}) + \\
&\quad ICF(G_{hc\leftrightarrow hc1}, G_{hc\leftrightarrow hc2}, S_{hc\leftrightarrow hc}) - L_{hc} O_{hc}(t) - K_{hc}) \qquad (2)\\
ICF(G_1, G_2, I) &= G_2 \tanh(G_1 I) \qquad (3)\\
ORF(I) &= \begin{cases} I & \text{if } I \geq 0 \text{ and } I \leq 1 \\ 1 & \text{if } I > 1 \\ 0 & \text{if } I < 0 \end{cases} \qquad (4)
\end{aligned}
$$

Where :

$S_{l\rightarrow c} \equiv$ *Incident light intensity*

$S_{c\leftrightarrow c} \equiv$ *Gaussian weighted sum of cone − to − cone inputsignals*

$S_{hc\rightarrow c} \equiv$ *Inverted − Gaussian weighted sum of HC − to − cone input signals*

$G_{l\rightarrow c1}, G_{l\rightarrow c2} \equiv$ *Incident light gain parameters*

$G_{c\leftrightarrow c1}, G_{c\leftrightarrow c2} \equiv$ *Cone − to − cone coupling strength*

$G_{hc\rightarrow c1}, G_{hc\rightarrow c2} \equiv$ *HC − to − cone coupling strength*

$L_c \equiv$ *Cone output dependent leakage modulation parameter*

$K_c \equiv$ *Constant cone leakage*

$S_{c\rightarrow hc} \equiv$ *Inverted − Gaussian weighted sum of cone − to − HC input signals*

$S_{hc\leftrightarrow hc} \equiv$ *Gaussian weighted sum of HC − to − HC input signals*

$G_{c\rightarrow hc1}, G_{c\rightarrow hc2} \equiv$ *Cone − to − HC coupling strength*

$G_{hc\leftrightarrow hc1}, G_{hc\leftrightarrow hc2} \equiv$ *HC − to − HC coupling strength*

$L_{hc} \equiv$ *HC output dependent leakage modulation parameter*

$K_{hc} \equiv$ *Constant HC leakage*

$I \equiv$ *Input signal strength*

$G_1 \equiv$ *Lumped pre − nonlinearity gain*

$G_2 \equiv$ *Lumped post − nonlinearity gain*

$ORF \equiv$ *Output signal half wave rectification function*

$ICF \equiv$ *Individual input signal non − linear transformer function*

$O_c \equiv$ *Network cone reponse function*

$O_{hc} \equiv$ *Network HC response function*

The light response of a cone pedicle $O_c(t+1)$ is computed by the Output Rectification

Function (ORF) as a rectified sum of the signals from its outer segment and neighboring pedicles minus the feedback signal from neighboring HC's and minus two leakages, one constant (K_c) and the other (L_c) output dependent (Eqn. 1). The leakage parameters were originally intended to model the effects of lumped cellular membrane leakage conductances and membrane voltage dependent leakge conductances. However, the leakage parameters can also be used to model various threshold effects and are used in such way in our simulations. The HC response $O_{hc}(t+1)$, is determined by inputs from neighboring pedicles and surrounding HC's (Eqn. 2).

In equations 1 and 2, all components representing input signals are characterized by a distinct Input Conductance Function (ICF). In case of synaptic signal transmission the ICF is a lumped characterization of the actual synaptic conductances that vary from synapse to synapse. This lumped characterization is adequate as we assume the overall cellular response is not very sensitive to individual synaptic variations. The input to an ICF is a Gaussian weighted sum of input signals.

The concept of signal propagation delay is not explicitly defined but rather implied in the model. The consequence is that all signal delays in the model are either zero or one simulation step. The use of implicit signal propagation delay allows for significantly faster simulation time and was introduced intentionally based on the assumption that the overwhelmingly dominant signal propagation delay in OPL is affected more by the chemical synapses between the pedicles and the HC's as opposed to electrical coupling between cells. This simplification also facilitates the analysis of the steady-state behavior of the model.

In all simulation studies a single layer of 128x128 cone pedicles was used. The size of the horizontal cell layer varied depending on the RF model being investigated (42x42 for DooG

and m-DooG and 128x128 for LoG and DoG). In the DooG and m-DooG experiments, the cone-to-HC convergence ratio was 9(Wässle, Gruner, Röhrenbeck, & Boycott, 1990; Kolb, 1974). Our model allows the spatial extent of the cone electrical coupling to be set anywhere from 128x128 to zero. In all simulations the central portion of the cone RF has a diameter of approximately 7 pedicles representing cone-to-cone coupling. The spatial extent of the negative feedback from HC's to pedicles is assumed to be the same as that of the pedicle-to-HC connections (1 pedicle to 1 HC for DoG and LoG and 1 pedicle to approximately 9 HC's for DooG and m-DooG). This assumption is partially supported by data that suggest the negative feedback from HC's to pedicles is mediated by specialized chemical processes rather than separate conventional synapses(Raviola & Gilula, 1975). Based on the inner diameter of the antagonistic surround of the cone RF (on the order of 50μm (Westheimer, 1967; Tulunay-Keesey & Jones, 1977)) and the cone-to-HC convergence ratio (9:1 for DooG and m-DooG and 1:1 for DoG and LoG)(Schein & DeMonasterio, 1987; Krebs & Krebs, 1989; Wässle et al., 1990), the extent of the gap junction mediated HC-to-HC coupling was estimated to span a diameter of approximately 7 HC's for DooG and m-DooG and 25 HC's for DoG and LoG. In the simulation studies, all spatial couplings have a Gaussian sensitivity profile except for the cone-to-HC and HC-to-cone connections where they are (1) inverted-Gaussians for m-DooG, (2) constant with a *hole* at the center for DooG, and (3) constant for DoG and LoG. Furthermore, as the Gaussian has an infinite spatial extent a truncated approximation was necessary in the model. The maximal spatial extent of the RF's along any axis is about 12 times the respective space constants thus the truncated approximation captures more than 99.9% of the integral of the Gaussian.

4.3 Simulation Results

The experiments conducted on the computational model were analogous to equivalent experiments designed to gather physiological data. A fixed intensity light stimulus of variable diameter was centered on the dark-adapted, cone layer that represents a patch of the fovea. The steady-state (400 ms from stimulus onset) cone and HC responses at the center of the spot were recorded.

[Insert Fig. 9 About Here]

Fig. 9 demonstrates the characteristic center-surround antagonism in cone response using various RF models. Due to balanced center-surround contribution, the LoG and DooG responses are inconsistent with the cone response data in Fig. 2. More realistic fit to data is provided by the DoG and m-DooG responses. The LoG cone reponse hyperpolarizes maximally at a smaller stimulus diameter than the other RF model responses due to the stronger contribution from a narrower surround dictated by the LoG formalism (see Fig. 3). For the same reason, the LoG response depolarizes at a steeper rate with respect to stimulus diameter than the other RF responses. The DoG and DooG responses are similar at small stimulus diameters but diverge at large stimulus diameters due to the unbalanced center-surround contribution in the DoG RF model. The m-DooG response has a steeper hyperpolarization, upto its maximum, with increasing stimulus diameter than the other RF responses due to its inverted-Gaussian RF basis. This effect is in turn reflected in the HC response as a shallower hyperpolarization rate, upto maximal response, with increasing stimulus size as show in Fig. 10.

The DoG and m-DooG responses at larger stimulus diameters are determined by the ratio between the center and surround RF zones. Although this ratio can be tuned over a certain range, there are fundamental limitations that are not obvious from steady-state responses. In conventional use of the DoG, LoG, and DooG RF models, the source of excitation for both the center (i.e. cones) and surround (i.e. HC's) is the stimulus. Of course, this is anatomically incorrect but it does allow for any tuning of the center-surround contribution ratio without considering system analysis and possibility of oscillation in cone response. In an anatomically correct model, cones are excited by the stimulus but the HC's are driven by cones and not the stimulus. In our simulations we found that it is impossible to have strong negative feedback from HC's to cones (e.g. balanced center-surround contribution) without introducing strong *ringing* in the cone response, even with large leakage conductances. This fact and the absence of strong oscillations in recorded cone responses further argue against balanced cone RF.

The HC reponse, using the four RF models, as a function of increasing stimulus diameter is shown in Fig. 10. The DoG, LoG, and DooG responses hyperpolarize with increasing stimulus diameter and saturate at large stimulus diameters. These responses are consistent with the Gaussian RF basis as shown in Fig. 4. On the contrary, the m-DooG HC response displays a small but definite center-surround antagonistic influence for larger stimulus diameters. It is not obvious that the antagonism is due to the inverted-Gaussian RF basis. But, it is the inverted-Gaussian RF basis that induces the antagonism in HC's through cones with increasing stimulus diameter. To visualize this process, imagine a central HC that receives inputs from cones mediated by an inverted-Gaussian RF basis. The HC response is maximally hyperpolarized when the cones that stimulate it are maximally hyperpolarized.

This is the case when the stimulus diameter is such that the cones in the periphery of the HC inverted-Gaussian RF basis are maximally stimulated. However, as stimulus diameter increases further the same cones depolarize as they receive stronger negative feedback signals from more eccentric HC's. A consequence of the antagonism in HC response is a shallower cone depolarization at larger stimulus diameters (compare the m-DooG and DoG responses in Fig. 9).

In summary, simulated cone and HC reponses (Fig. 9 and Fig. 10) show m-DooG is the only RF model that can account for known OPL anatomy and physiology (Fig. 2 and Fig. 6).

[Insert Fig. 10 About Here]

5 Discussion

Intracellularly recorded light responses from cones and narrow field HC's in the Tiger salamander retina were used to evaluate several RF models (i.e. DoE, DoG, LoG, DooG, m-DooG, and Gabor) as approximation to the antagonistic center-surround configuration of cone RF. Computational model of the primate OPL was utilized to help to discriminate among the RF models.

Analytically, the antagonistic contribution from center and surround (Fig. 2) could be approximated by the DoG function. This model however can not explain why HC's also display center-surround antagonism. Anatomical evidence suggests that HC's contact cones through invaginating processes that are lateral in the cone ribbon synapse(Rodieck, 1973); there is no clear distinction between feedback and feedforward direction of synaptic transmission. How could then HC, respond to an annulus with membrane depolarization, reflecting

activities of a cone, that is concentric with HC's dendritic field, while at the same time being hyperpolarized by neighboring HC's responding directly to the annulus? One possibility is that different HC types, not coupled electrically, provide separate feedback pathways to cone pedicles. It is now believed that all vertebrates have at least two types of HC's(Gallego, 1983, 1986; Rodieck, 1988). Two morphological types of HC were reported in Ambystoma Tigrinum, one axonless and the other having both cell body and the axon terminal (AT) (Lasansky & Vallerga, 1975). Of course any conclusion based on Golgi stain must be accepted with caution since the HC axons are at times only a fraction of a micron in diameter and could be hard to impregnate. It is also possible that the narrow field HC's which display clear center-surround antagonism are the cell bodies while the AT with their very large RF provide the feedback pathway. This can be discounted in primates where type I HC AT's contact only rods(Boycott, Hopkins, & Sperling, 1987; Wässle et al., 1989). Another possibility is the chromaticity HC's in the fish(Stell, 1976). However, in the primate retina only luminosity HC types are observed (Boycott et al., 1987; Wässle et al., 1989). Our simulations suggest that explanation of the center-surround antagonism observed in HC's does not require separate HC feedback pathways to cone pedicles.

The effect of inverted-Gaussian sensitivity profile of the feedback from HC dendritic field is to introduce a spatial phase shift of the maximal signal conduction path from cones to HC's. In other words, cone response to a point stimulus is maximized while the concentric HC remains unexcited. From signal processing point of view, the configuration increases the spatial frequency response bandwidth of the system. Since cone signals are smoothed and blurred somewhat due to electrical coupling, it can be argued that such a phase shift in cone and HC connectivity serves to deblur high spatial frequency signals while maintaining

system noise immunity. Assuming our prediction of smooth synaptic density distribution over the extent of the HC DF is correct, our model is consistent with the hypothesis that Gaussian spatial smoothing (i.e. smoothing with good signal localization characteristics) is optimal(Marr, 1982) as opposed to simple averaging (e.g. boxcar). Our model is also compatible with the two general views on the function of lateral inhibition in vision, namely redundancy removal (dynamic range expansion)(Barlow, 1961a, 1961b) and deblurring(Ratliff, 1965). Additionally, in as far as cones report relative contrast information, our model reduces the probability of spurious operating point changes (i.e. shifting of the cone operating curve) by comparing the illuminance at a given point to that of its surround and not to itself. Similarly, the efficiency of the spatial deblurring operation is improved as the mechanism correctly emphasizes difference between luminances at spatially offset points. Finally, the m-DooG model is also compatible with the spatial frequency response equalization interpretation of deblurring(Georgeson & Sullivan, 1975) as it selectively boosts the system reponse to high spatial frequency stimuli.

5.1 Perceptual Correlates

The perceptual correlates of the hypothesized mechanism are more difficult to ascertain. If the effect is manifested at the perceptual level, then it would seem that for high spatial frequency stimuli (e.g. stimuli with smaller diameter than that of the HC DF), the perceived lightness would increase rapidly with stimulus size upto diameter where feedback becomes effective. On the other hand, for larger stimuli, perceived lightness would probably still increase but at a slower rate than for smaller stimuli as negative feedback from HC's is activated. Based on the inverted-Gaussian model of the feedback from HC, less than 5% of

the total feedback signal strength is due to stimuli within a diameter less than half that of the HC DF (i.e. the central 4σ region). This prediction is consistent with psychophysical studies of Ricco's law and spatial frequency response observed in the fovea(Graham & Bartlett, 1939, 1940; Bartlett, 1965; Wald, 1938).

Direct correlations between physiological and psychophysical data are often tenuous with perhaps the exception of psychophysical studies of foveal vision using small stimuli. In the fovea, the spatial resolution of single cones is preserved throughout the visual processing stages thus minimal distortions exist between physiologically measured cell responses and psychophysically observed behavior. Psychophysical experiments(Graham & Bartlett, 1939, 1940; Bartlett, 1965; Wald, 1938) show that there are two *knees* in the foveal cone response versus stimulus diameter response curve, one at about 20 μm and the other at 60 μm which correspond well with the widths of primate foveal HC and cholinergic amacrine cell DF's respectively(Wässle et al., 1989; Wässle & Boycott, 1991).

Our model is also consistent with the observation(Stevens, 1961) that with increasing illumination, lightness of a grey surface becomes lighter while lightness of a black surface decreases (see also Jameson & Hurvich, 1961). The center-surround interactions at the OPL cause the I-R curve of every single cone to be shifted in intensity domain until it is in register with ambient light(Skrzypek, 1990a). The slope of the simulated I-R curves increases with intensity(Skrzypek & Wu, 1992). Consequently, absolute difference between luminance of light grey and dark grey will produce smaller response on the steep I-R curves in the dim light and larger response on the shallower I-R curve shifted towards higher intensity domain.

Our model can also partially account for some areal contrast phenomena including modification of a target color by the surround (Brou et al 1986) and the effect of contrast on

perception of brightness (Shapley & Reid 1985) Fig. 11 shows the behavior of the simulated cones in response to a spot of light that spans more than 50 cones in diameter. Initially all cones generate a peak response, but after 50 to 100 msec there is a redistrubution of membrane potentials in different cones depending on their position under the stimulus. Cones at the edge of the stimulus are more hyperpolarized than cones toward the center. This is an expected consequence of the antagonistic lateral interactions within OPL. Thus depending on the position of a cone with respect to luminance discontinuity the response could be larger or smaller than what would be expected from the I-R curve of a single cone.

[Insert Fig. 11 About Here]

Despite evidence of theoretical advantages and perceptual correlates, the functional significance of the hypothesized mechanism remains a topic for further investigations. Nevertheless, it has been demonstrated that (1) there are experimental grounds to reject many of the classical RF models and (2) m-DooG is the only quantitative RF model that can account for known physiology and anatomy of the OPL.

A Analytical Foundation

The rudiments of light response in an isolated cone is now fairly well understood. For a selected light intensity range the isolated cone response can be characterized by Eqn. 6. We build upon this foundation a general conceptualization of how a network cone(i.e. cone in the retina) respond to light. The light response observed at a cone pedicle(Eqn. 9) is a weighted sum of the signals from the cone outer segment(Eqn. 5) and the neighboring cones($V_{ic}\,'s \otimes G_{nc \leftrightarrow nc}$) minus a weighted sum of signals from the surrounding neighboring HC's($V_{nhc}\,'s \otimes G_{hc \rightarrow ic}$).

$$
\begin{aligned}
F_{os} &\equiv \textit{Isolated cone outer segment light response} \\
&= \int I(\lambda)S(\lambda)d\lambda && (5) \\
V_{ic} &\equiv \textit{Isolated cone pedicle light response} \\
&= V_{max}\frac{F_{os}^{n}}{F_{os}^{n}+K} && (6) \\
G(x,y,\sigma_x,\sigma_y) &\equiv \textit{Generalized 2D Gaussian receptive field} \\
&= \frac{1}{2\pi\sigma_x\sigma_y}\exp^{-0.5(\frac{x^2}{\sigma_x^2}+\frac{y^2}{\sigma_y^2})} && (7) \\
IG(x,y,\sigma_x,\sigma_y) &\equiv \textit{Generalized 2D inverted} - \textit{Gaussian receptive field} \\
&= \frac{1}{2\pi\sigma_x\sigma_y}(1-\exp^{-0.5(\frac{x^2}{\sigma_x^2}+\frac{y^2}{\sigma_y^2})}) && (8) \\
V_{nc} &\equiv \textit{Network cone response to light} \\
&= V_{ic}\,'s \otimes G_{nc \leftrightarrow nc} - V_{nhc}\,'s \otimes IG_{hc \rightarrow ic} && (9) \\
&\quad \textit{Where}: \\
&\quad\quad G_{nc \leftrightarrow ic} \textit{ represents cone to cone gap junction coupling.} \\
&\quad\quad IG_{hc \rightarrow ic} \textit{ represents HC to cone feedback signal gain.} \\
V_{nhc} &\equiv \textit{Network horizontal cell response} \\
&= V_{nc}\,'s \otimes IG_{nc \rightarrow hc} + V_{hc}\,'s \otimes G_{hc \leftrightarrow hc} && (10) \\
&\quad \textit{Where}: \\
&\quad\quad IG_{nc \rightarrow hc} \textit{ represents cone to HC feedforward signal gain.} \\
&\quad\quad G_{hc \leftrightarrow hc} \textit{ represents HC to HC gap junction coupling.}
\end{aligned}
$$

$$
\begin{aligned}
\lambda &\equiv \textit{Incident light wavelength} \\
I(\lambda) &\equiv \textit{Incident spectral intensity} \\
S(\lambda) &\equiv \textit{Spectral sensitivity function} \\
V_{max} &\equiv \textit{Saturating light response level} \\
n &\equiv \textit{Normalizing exponent} \\
K &\equiv \textit{Half-intensity adaptation constant}
\end{aligned}
$$

Reference

Attwell, D., Werblin, F., & Wilson, M. (1982). The Properties of Single Cones Isolated from the Tiger Salamander Retina. *J. of Physiol., 328*, 259–283.

Barlow, H. B. (1961a). Possible Principles Underlying the Transformation of Sensory Messages. In Rosenlith, R. A. (Ed.), *Sensory Communication*, pp. 217–234. MIT Press, Cambridge,Massachusetts.

Barlow, H. B. (1961b). Three Points about Lateral Inhibition. In Rosenblith, R. A. (Ed.), *Sensory Communication*, pp. 782–786. MIT Press, Cambridge, Massachusetts.

Bartlett, N. R. (1965). Thresholds as Dependent on Some Energy Relations and Characteristics of the Subject. In Graham, C. H. (Ed.), *Vision and Visual Perception*, chap. 7, pp. 154–184. John Wiley and Sons, New York, New York.

Baylor, D., Fuortes, M., & O'Bryan, P. (1971). Receptive Fields of Single Cones in the Retina of the Turtle. *J. Physiol, 214*, 265–294.

Boycott, B., Hopkins, J., & Sperling, H. (1987). Cone Connections of the Horizontal Cells of the Rhesus Monkey's Retina. *Proc. R. Soc. Lond. B, 229*, 345–379.

Burkhardt, D. (1977). Responses and receptive field organizations of cones in perch retinas. *J. Neurophysiol, 40*, 53–62.

Daugman, J. (1980). Two-Dimensional Spectral Analysis of Cortical Receptive Field Profiles. *Vision Research, 20*, 847–856.

Gallego, A. (1983). Organization of the Outer Plexiform Layer of the Tetrapoda Retina. *Prog. Sens. Physiol.*, *4*, 83–114.

Gallego, A. (1986). Comparative Studies on Horizontal Cells and a Note on Microglial Cells. *Prog. Ret. Res.*, *5*, 165–206.

Georgeson, M., & Sullivan, G. (1975). Contrast Constancy: Deblurring in Human Vision by Spatial Frequency Channels. *J. Physiol.*, *252*, 627–656.

Graham, C. H., & Bartlett, N. R. (1939). The Relation of Size of Stimulus and Intensity in the Human Eye: II. Intensity Thresholds for Red and Violet Light. *J. Exp. Psychol.*, *24*, 574–587.

Graham, C. H., & Bartlett, N. R. (1940). The Relation of Size of Stimulus and Intensity in the Human Eye: III. The Influence of Area on Foveal Intensity Discrimination. *J. Exp. Psychol.*, *25*, 149–159.

Kaneko, A. (1970). Physiological and morphological identification of horizontal, bipolar and amacrine cells in goldfish retina. *J. Physiol*, *207*, 623–633.

Kolb, H. (1974). The connections between horizontal cells and photoreceptors in the retina of the cat. *J. Comp. Neurol.*, *155*, 1–14.

Krebs, W., & Krebs, I. P. (1989). Quantitative Morphology of the Central Fovea in the Primate Retina. *Am. J. Anatomy*, *184*, 225–236.

Lasansky, A. (1978). Contacts between Receptors and Electrophysiologically Identified Neurones in the Retina of the Larval Tiger Salamander. *J. Physiol.*, *285*, 531–542.

Lasansky, A. (1981). Synaptic Action Mediating Cone Responses to Annular Illumination in the Retina of the Larval Tiger Salamander. *J. Physiol.*, *310*, 205–214.

Lasansky, A., & Vallerga, S. (1975). Horizontal Cell Responses in the Retina of the Larval Tiger Salamander. *J. Physiol.*, *251*, 145–165.

Marr, D. (1982). *Vision: A Computational Investigation into the Human Representation and Processing of Visual Information.* Freeman, San Francisco, California.

Marr, D., & Hildreth, E. (1980). Theory of Edge Detection. *Proc. R. Soc. London B*, *207*, 187–217.

Marshall, L., & Werblin, F. (1978). Synaptic inputs to the horizontal cells in the retina of the larval tiger salamander. *J. Physiol.*, *279*, 321–346.

Ratliff, F. (1965). *Mach Bands: Quantitative Studies on Neural Networks in the Retina.* Holden-Day, San Francisco.

Raviola, E., & Gilula, B. (1975). Intramembrane Organization of Specialized Contacts in the Outer Plexiform Layer of the Retina. *J. Cell Biol.*, *65*, 192–222.

Rodieck, R. W. (1965). Quantitative Analysis of Cat Retinal Ganglion Cell Response to Visual Stimuli. *Vision Research*, *5*, 583–601.

Rodieck, R. W. (1973). *The Vertebrate Retina: Principles of Structure and Function.* W. H. Freeman and Company, San Francisco.

Rodieck, R. (1988). The Primate Retina. In Steklis, H. D., & J., E. (Eds.), *Comparative Primate Biology Volume 4: Neurosciences*, pp. 203–278. Alan R. Liss, Inc., New York.

Schein, S. J., & DeMonasterio, F. M. (1987). The Mapping of Retinal and Geniculate Neurons onto Striate Cortex of Macaque. *J. Neurosci.*, *7*, 996–1009.

Skrzypek, J. (1984). Electrical Coupling Between Horizontal Cell Bodies in the Tiger Salamander Retina. *Vision Research*, *24*(4), 701–711.

Skrzypek, J. (1990a). Feedback Synapse to Cone and Light Adaptation. In Touretzky, D. (Ed.), *Advances in Neural Information Processing Systems, NIPS 3* San Mateo, CA. Morgan Kaufman.

Skrzypek, J. (1990b). Light sensitivity in cones is affected by the feedback from horizontal cells. In Eeckman, F. (Ed.), *Analysis and Modeling of Neural Systems.* Kluwer Academic.

Skrzypek, J., & Werblin, F. (1978). All Horizontal Cells Have Center-Surround Antagonistic Receptive Fields. *ARVO Abstr.*, *1*, 1.

Skrzypek, J., & Wu, G. (1992). Computational model of invariant contrast adaptation in the outer plexiform layer of the vertebrate retina. In Eeckman, F. (Ed.), *Computational Neural Systems CNS*92.* Kluwer Academic.

Skrzypek, J. (1979). *Synaptic Mechanism of the Light Response in Horizontal Cells of the Tiger Salamander Retina.* Ph.D. thesis, University of California, Berkeley.

Skrzypek, J., & Werblin, F. (1983). Lateral Interactions in Absence of Feedback to Cones. *J. Neurophysiol.*, *49*, 1007–1016.

Stell, W. (1976). Functional Polarization of Horizontal Cell Dendrites in Goldfish Retina. *Invest. Ophthal. Visual Sci.*, *15*, 895–907.

Stevens, S. (1961). To Honor Fechner and Repeal His Law. *Science*, *133*, 80–86.

Stewart, W. (1978). Functional connections between cells as revealed by dye-coupling with a highly fluorescent napthalimide tracer. *Cell*, *14*, 741–759.

Tulunay-Keesey, U., & Jones, R. M. (1977). Spatial Sensitization as a Function of Delay. *Vision Research*, *17*, 1191–1199.

Wald, G. (1938). Area and Visual Threshold. *J. Gen. Physiol.*, *21*, 269–287.

Wässle, H., Boycott, B., & Röhrenbeck, J. (1989). Horizontal Cells in the Monkey Retina: Cone Connnections and Dendritic Network. *Eu. J. Neurosci*, *1*, 421–435.

Wässle, H., Gruner, U., Röhrenbeck, J., & Boycott, B. (1990). Retinal Ganglion Cell Density and Cortical Magnification Factor in the Primate. *Vision Research*, *30*, 1897–1911.

Wässle, H., & Boycott, B. B. (1991). Functional Architecture of the Mammalian Retina. *Physiological Review*, *71*(2), 447–480.

Werblin, F. (1978). Integrative pathways in local circuits between slow potential cells in the retina. *The Neurosciences*, *279*, 193–210.

Werblin, F., & Dowling, J. (1969). Organization of the Retina of the Mudpuppy, *Necturus maculosus*. II. Intracellular Recording. *J. Neurophysiol*, *32*, 339–355.

Westheimer, G. (1967). Spatial Interaction in Human Cone Vision. *J. Physiol.*, *190*, 139–154.

Young, R. (1985). The Gaussian Derivative Theory of Spatial Vision: Analysis of Cortical Cell Receptive Field Line-weighting Profiles. Tech. rep. GMR-4920, General Motors Research Lab Research Publication.

Young, R. A. (1987). The Gaussian Derivative Model for Spatial Vision: I. Retinal Mechanisms. *Spatial Vis.*, *2*, 273–293.

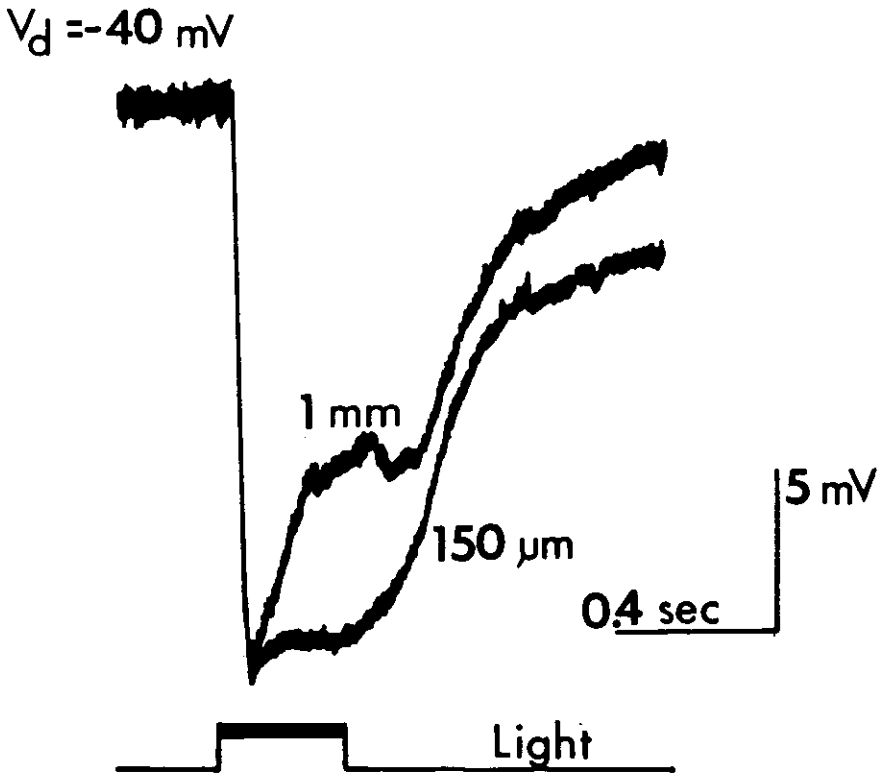

Figure 1: Intracellular cone responses to different diameter spots of white light (-3 LU). Overlaid peak responses to both 0.15 mm and to 1 mm spots are identical in amplitude (about 20 mV). However the hyperpolarization during the plateau of the response was decreased by 5 mV for large stimulus. At the offset of the large stimulus, there was additional transient hyperpolarization of about 1.5 mV.

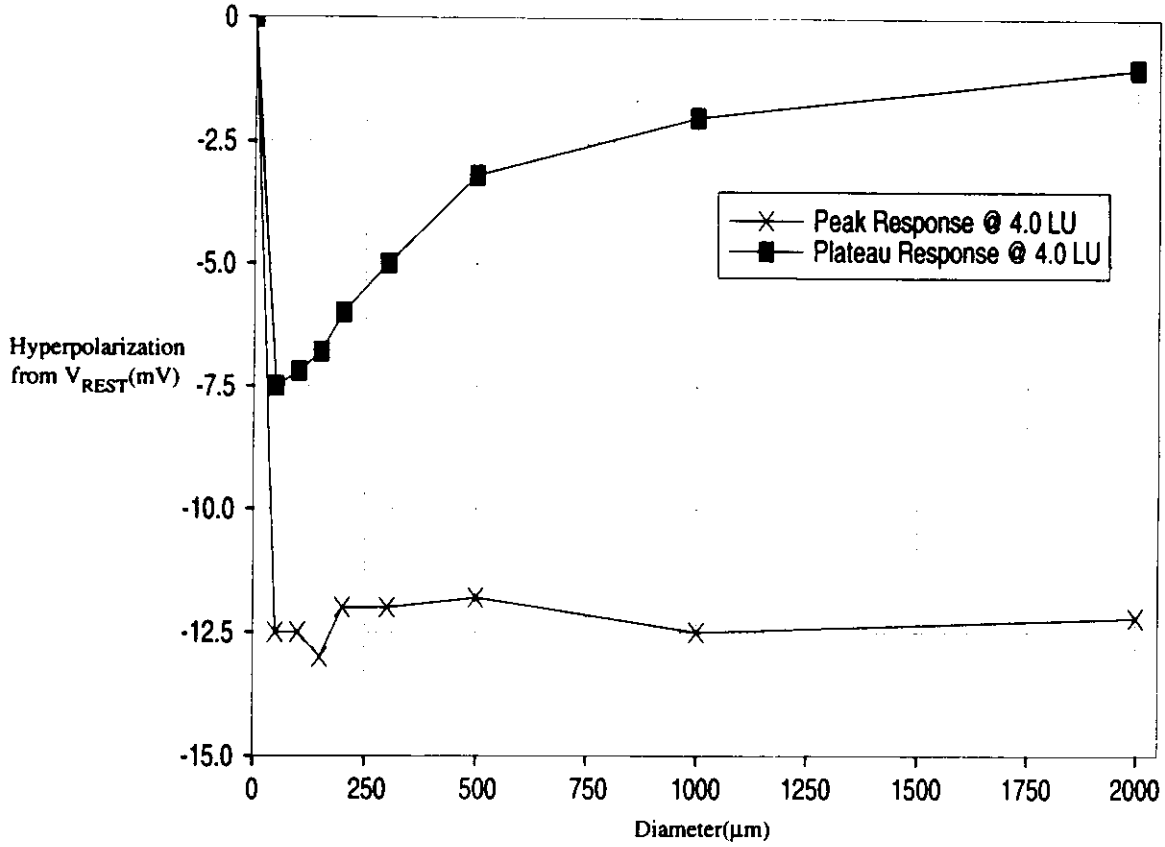

Figure 2: Intracellularly recorded red cone hyperpolarization from resting membrane potential(V_{REST}=-40 mV) versus the spot diameter of the stimulating white light at -4 LU. The peak response reached maximum at about 0.06 mm diameter and remained constant with increases in diameter up to 2.0 mm. The plateau response appears to decrease continuously with spot diameter but does not reach the resting level of the membrane.

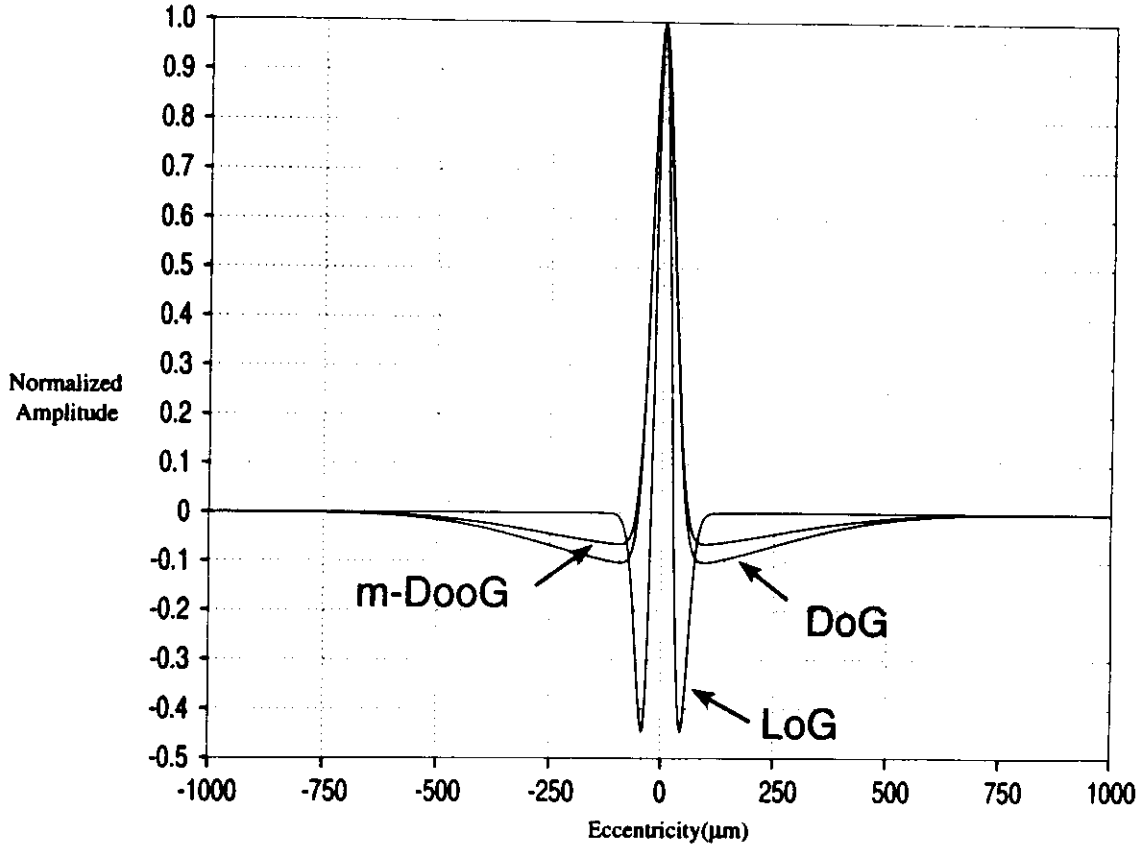

Figure 3: Typical sensitivity profile of the DoG, LoG, and m-DooG RF models with the same central zone space constant but different contribution and spatial extent of the surround zone. The surround in LoG is quite narrow in spatial extent and has a maximum contribution comparable to that of the center. Similarly, the DoG center-surround contribution is also balanced but the surround zone is much broader than that in LoG. The m-DooG surround zone is also very broad but its maximum contribution is small compared to that of the central zone. The actual equations for the profiles shown are as follows. $DoG(x) = \frac{10\exp^{-\frac{x^2}{1250}} - \exp^{-\frac{x^2}{125000}}}{9}$. $LoG(x) = \frac{0.0016\exp^{-\frac{x^2}{125}} - (0.0016x)^2\exp^{-\frac{x^2}{125}}}{0.0016}$. $DooG(x) = \frac{30\exp^{-\frac{x^2}{1250}} - \exp^{-\frac{(x-50)^2}{125000}} - \exp^{-\frac{(x+50)^2}{125000}}}{28.039603}$.

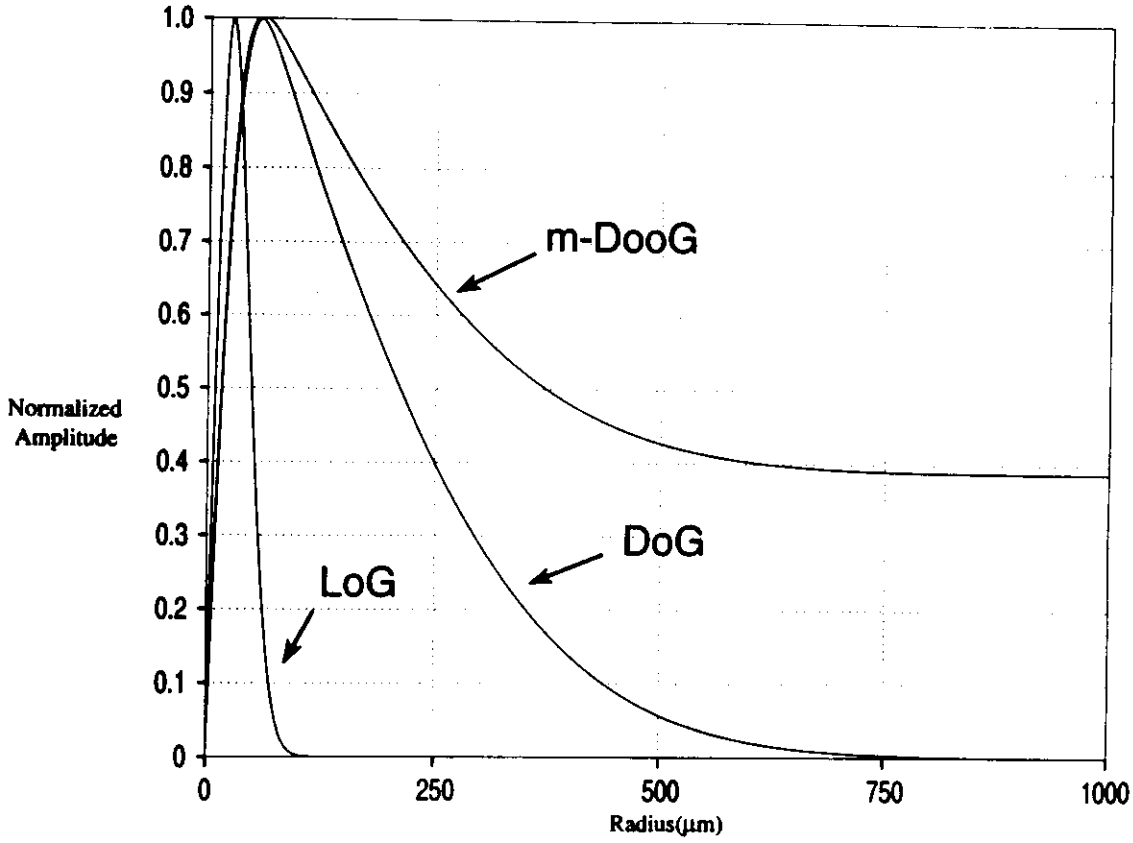

Figure 4: The amplitude spectrum of the RF sensitivity profiles. The m-DooG model has a non-zero DC sensitivity because of its unbalanced center and surround contribution as shown. Although shown here as having zero DC sensitivity, the DoG model can also be configured to have a non-zero DC sensitivity. On the contrary, the LoG model is defined to have zero DC sensitivity.

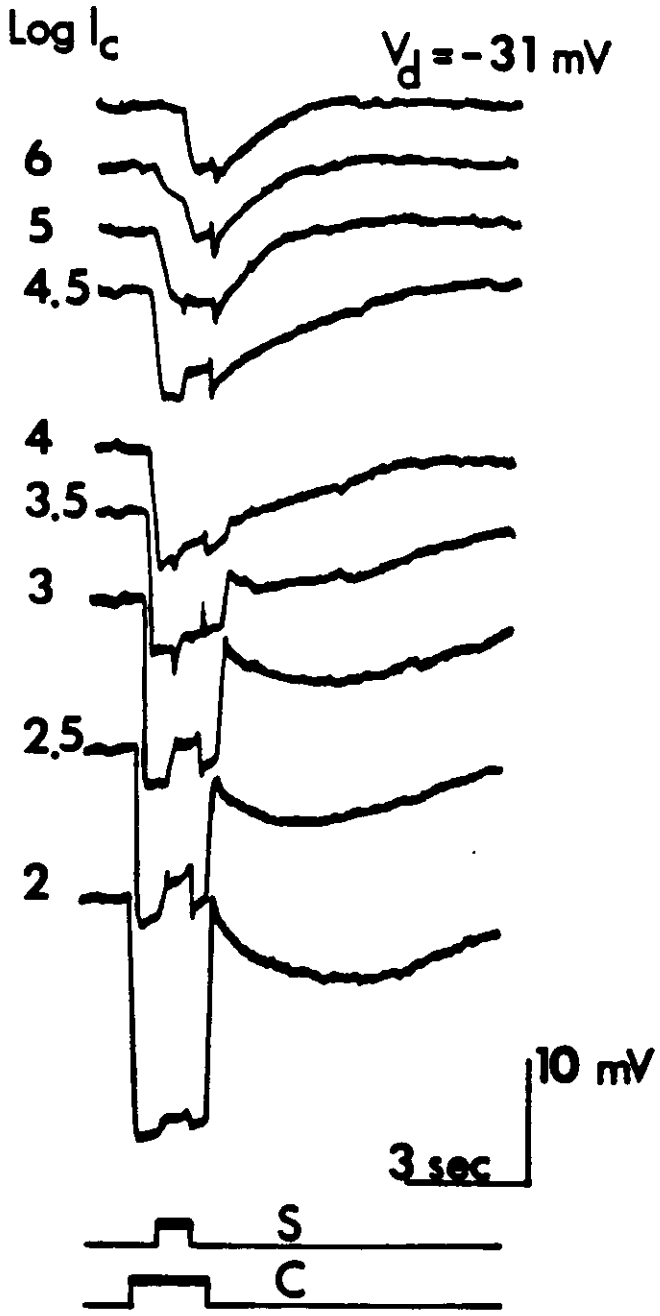

Figure 5: Intracellular responses recorded from the narrow field HC to various combinations of center-surround light intensity difference. The uppermost trace is a response to annulus alone (ID=1mm, OD=2mm) fixed at -3.2 LU. Numbers on the left side of each trace represent increasing intensities of the 0.5 mm spot of light. Note the increase in depolarization due to annulus at -4.5 LU followed by a decrease and a consequent second increase at -2.5 LU.

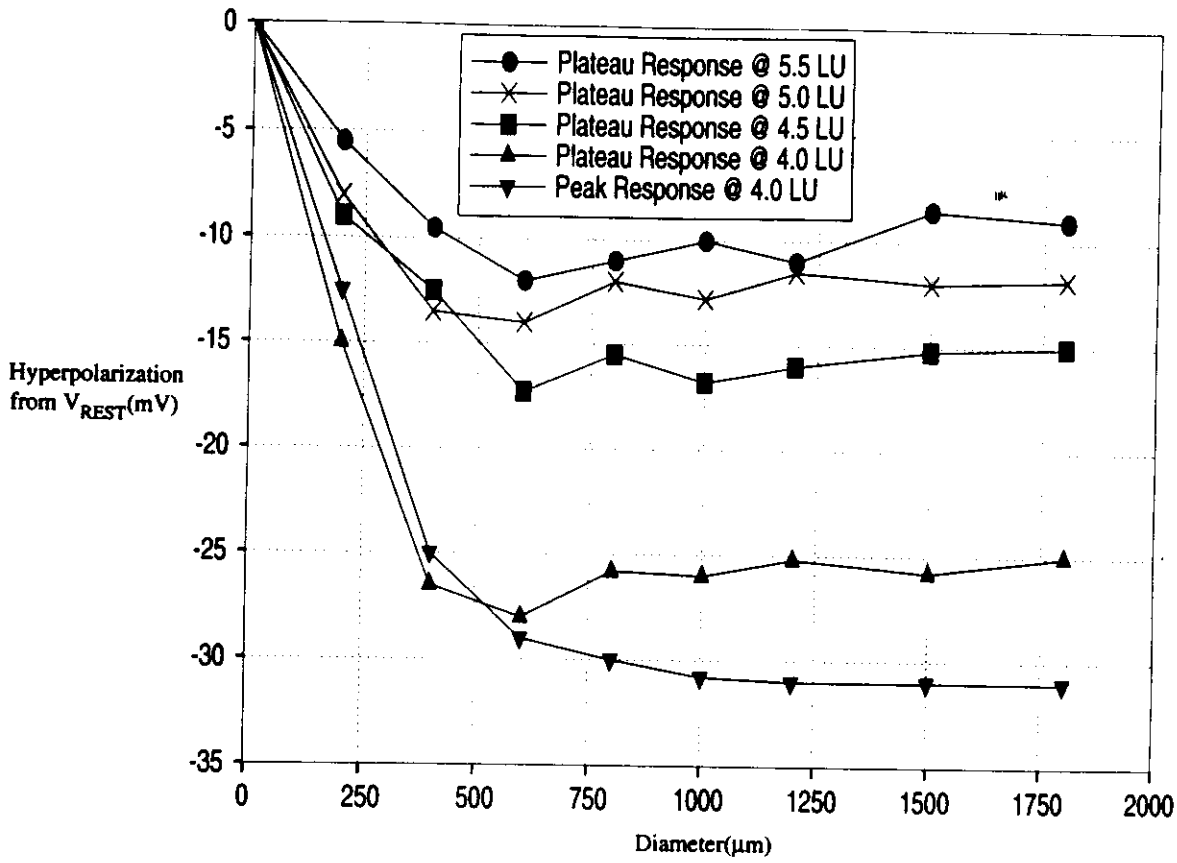

Figure 6: Intracellular light responses recorded from narrow field HC response versus diameter of the spot stimulus. Membrane potential in the dark(V_{REST}) is -25 mV. Peak response at 4 LU (filled down triangles) is larger than the plateau response (filled up triangles) at the same light intensity. This suggests that with increasing diameter plateau response is antagonized. The effect is also visible at lower intensities of the stimulus.

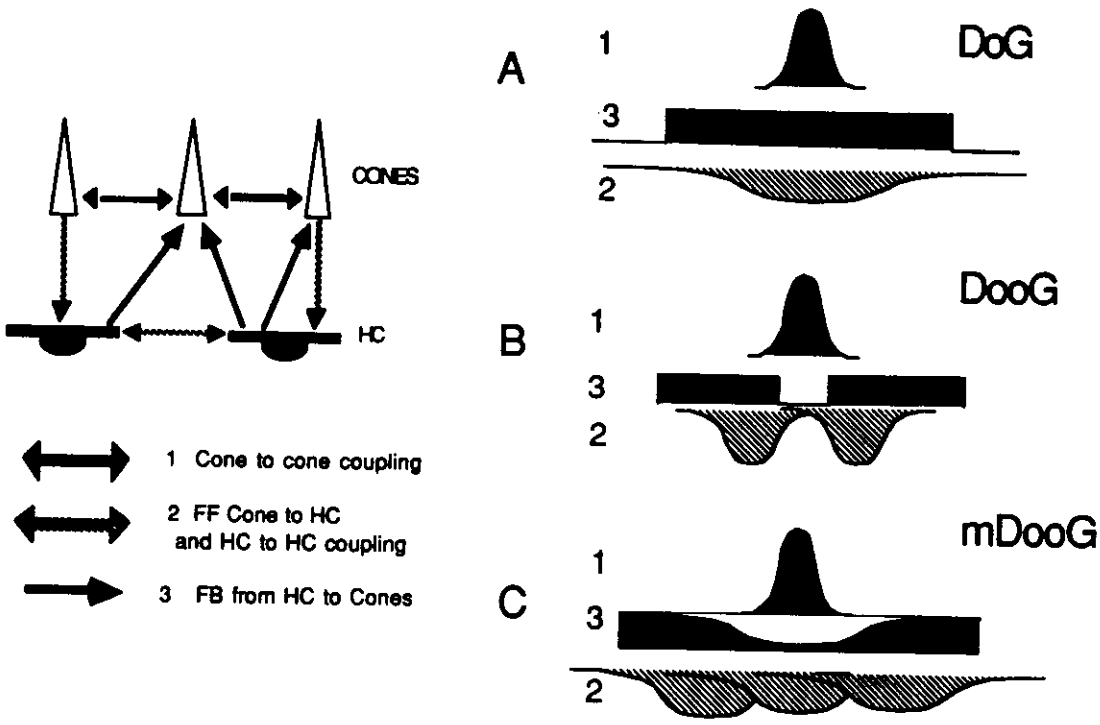

Figure 7: The schematic of synaptic interactions in the OPL (left) and three alternative models of the cone receptive field (right). RF models can be decomposed into Gaussian bases with different surround to center sensitivity profile. DoG (A) has a constant non-zero surround to center sensitivity profile; small positive Gaussian represents coupling between cones while the negative Gaussian represents HC RF including input from cones and coupling between HC's. DooG (B) has a constant non-zero surround to center sensitivity profile everywhere except at the very center where the sensitivity is zero, and m-DooG (C) has an inverted-Gaussian surround to center sensitivity profile.

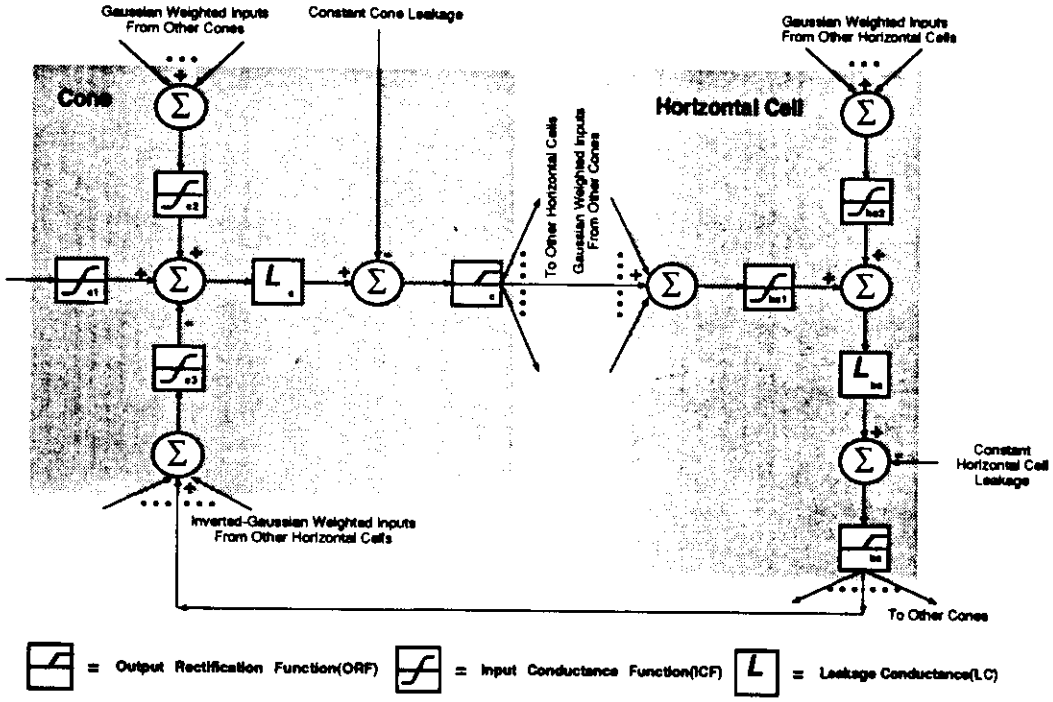

Figure 8: Functional diagram of the OPL model showing the the signal pathways and transformations using the m-DooG RF model.

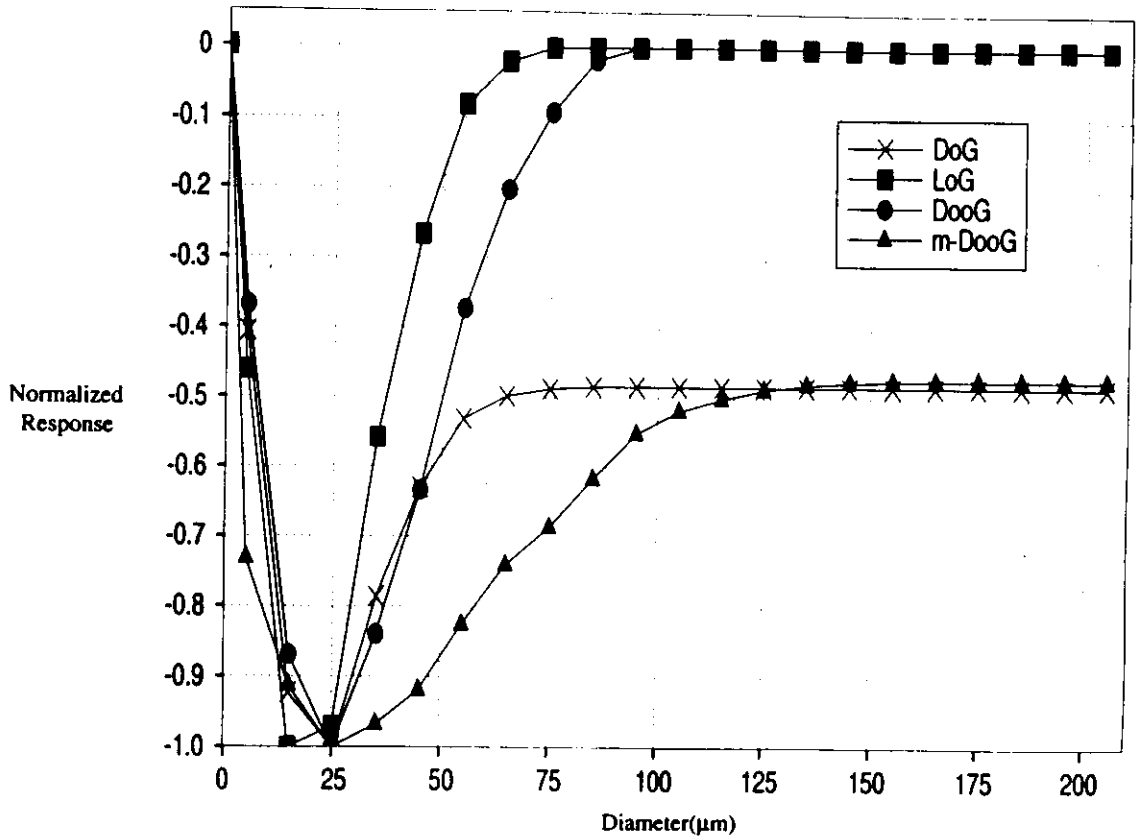

Figure 9: Simulated cone steady state light responses as a function of the spot diameter. When the cone receptive field is modeled as LoG (filled squares) or DooG (filled circles) functions, zero DC sensitivity is observed due to balanced center-surround contribution. The non-zero m-DooG model response (filled up triangles) at larger stimulus diameters clearly demonstrates the effects of unbalanced center-surround contribution.

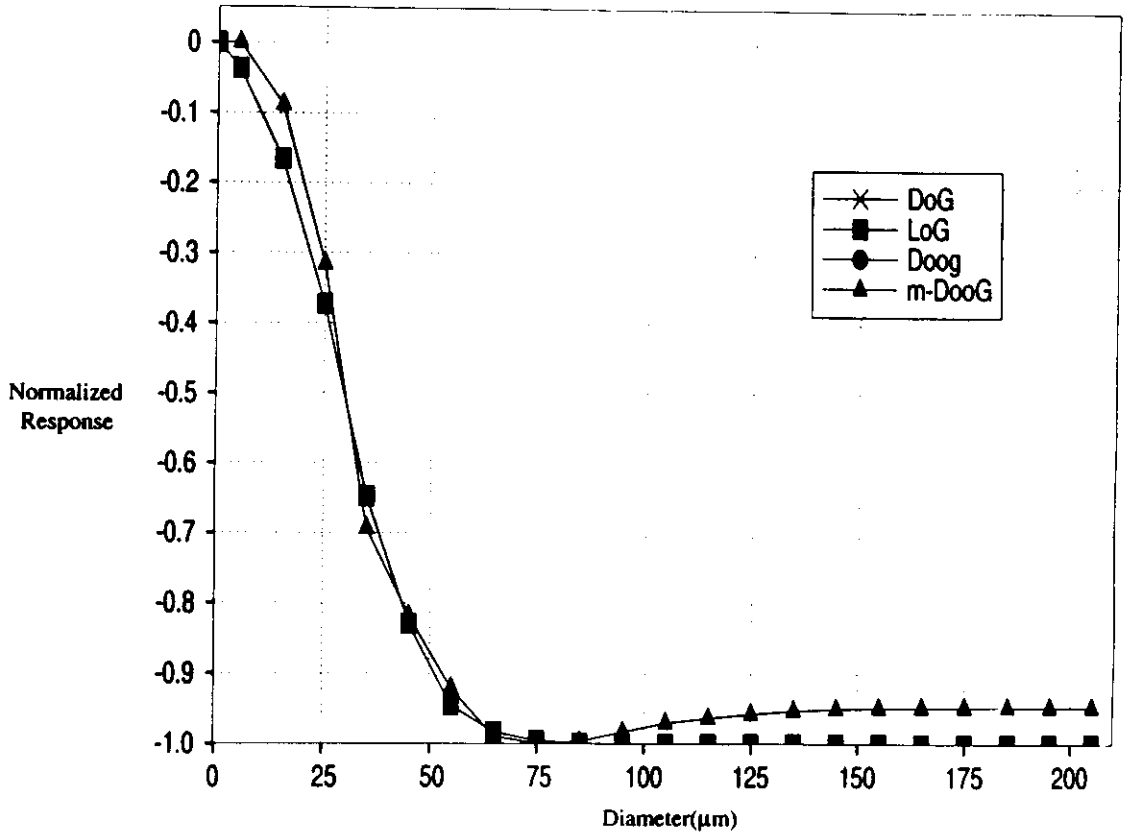

Figure 10: Steady state light response of simulated type I HC and plotted as a function of the stimulus diameter. Only the m-DooG model response (filled up triangles) demonstrates center-surround antagonism as shown by its maximal response at about 0.0075 mm and smaller responses at larger stimulus diameters.

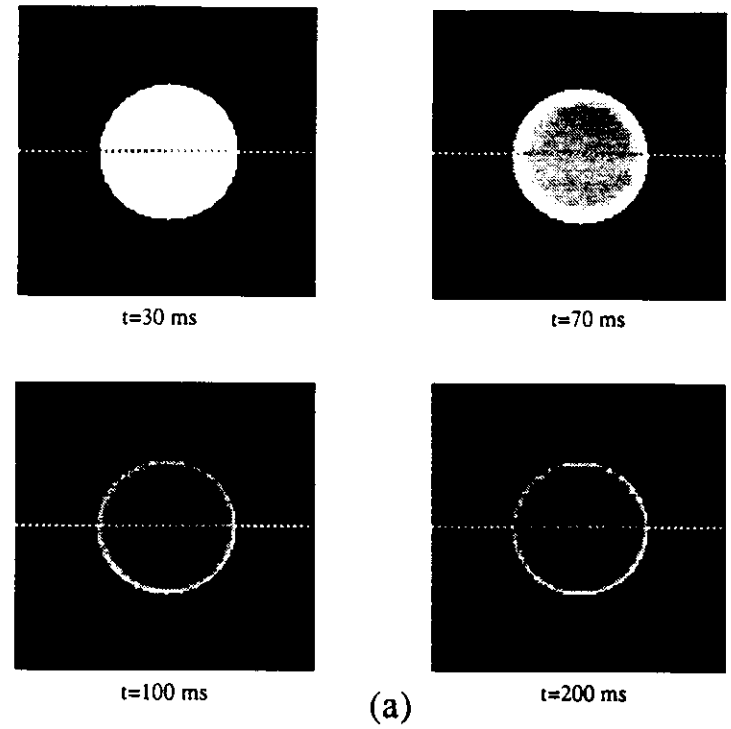

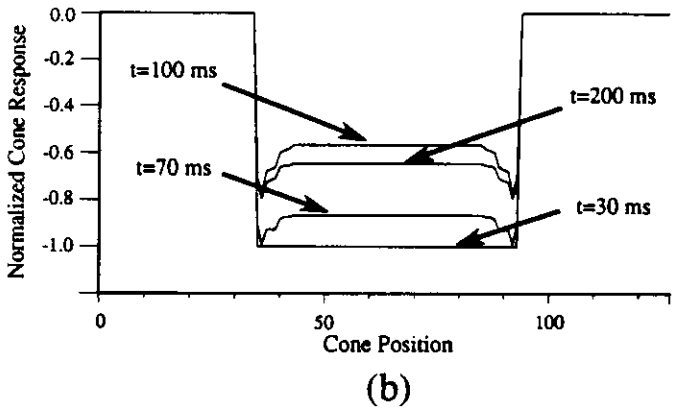

Figure 11: (A). The response of an array of cones(128x128) to a spot stimulus at various times since stimulus onset. The grey level of individual pixels within the circle represent the amplitude of the individual cone light responses. The equivalent light intensity was set to produce just-saturating peak response in cones. After 70 msec, a clear brighter ring is observed at the edge of the cricle. (B). The profile of cone responses measured along the dashed line indicated in (A). Maximal hyperpolarization is shown for the cones that are situated at the boundarties of the stimulus. The effect of feedback at the center of the circle corresponds to smaller hyperpolarization and is manifested in (A) as darker grey level.